# Conversion to the amyotrophic lateral sclerosis phenotype is associated with intermolecular linked insoluble aggregates of SOD1 in mitochondria

Han-Xiang Deng*†, Yong Shi*, Yoshiaki Furukawa‡, Hong Zhai*, Ronggen Fu*, Erdong Liu*, George H. Gorrie*, Mohammad S. Khan*, Wu-Yen Hung*, Eileen H. Bigio§, Thomas Lukas¶, Mauro C. Dal Canto§, Thomas V. O'Halloran‡, and Teepu Siddique*†‖**

*Davee Department of Neurology and Clinical Neurosciences, ‡Department of Chemistry, §Department of Pathology, Division of Neuropathology, ¶Department of Molecular Pharmacology and Biological Chemistry, ‖Department of Cell and Molecular Biology, and **Northwestern University Institute for Neuroscience, Northwestern University Feinberg School of Medicine, Tarry Building, Room 13-715, 303 East Chicago Avenue, Chicago, IL 60611

Communicated by Laszlo Lorand, Northwestern University Feinberg School of Medicine, Chicago, IL, March 16, 2006 (received for review January 16, 2006)

**Twenty percent of the familial form of amyotrophic lateral sclerosis (ALS) is caused by mutations in the Cu, Zn-superoxide dismutase gene (*SOD1*) through the gain of a toxic function. The nature of this toxic function of mutant SOD1 has remained largely unknown. Here we show that WT SOD1 not only hastens onset of the ALS phenotype but can also convert an unaffected phenotype to an ALS phenotype in mutant SOD1 transgenic mouse models. Further analyses of the single- and double-transgenic mice revealed that conversion of mutant SOD1 from a soluble form to an aggregated and detergent-insoluble form was associated with development of the ALS phenotype in transgenic mice. Conversion of WT SOD1 from a soluble form to an aggregated and insoluble form also correlates with exacerbation of the disease or conversion to a disease phenotype in double-transgenic mice. This conversion, observed in the mitochondrial fraction of the spinal cord, involved formation of insoluble SOD1 dimers and multimers that are crosslinked through intermolecular disulfide bonds via oxidation of cysteine residues in SOD1. Our data thus show a molecular mechanism by which SOD1, an important protein in cellular defense against free radicals, is converted to aggregated and apparently ALS-associated toxic dimers and multimers by redox processes. These findings provide evidence of direct links among oxidation, protein aggregation, mitochondrial damage, and SOD1-mediated ALS, with possible applications to the aging process and other late-onset neurodegenerative disorders. Importantly, rational therapy based on these observations can now be developed and tested.**

crosslinked | disulfide bonds | oxidation | protein aggregation | neurodegeneration

Amyotrophic lateral sclerosis (ALS) is a progressive paralytic disorder caused by degeneration of the motor neurons in brain and spinal cord (1). Most of the ALS cases are sporadic, with ≈5–10% being familial. The progressive paralysis in ALS usually affects respiratory function, leading to ventilatory failure and death; 50% of patients die within 3 years of onset of symptoms, and 90% die within 5 years. The juvenile form of ALS usually has a prolonged course of two to four decades. There is no known effective treatment for this fatal disease, although marginal delay in mortality has been noted with the drug riluzole (2).

Familial ALS can be transmitted as either a dominant or a recessive trait. We and our collaborators have previously shown that mutations in the Cu, Zn-superoxide dismutase gene (*SOD1*) are associated with ≈20% of familial ALS cases (3, 4). The pathogenic mechanisms underlying this disease are still largely unknown. Most, but not all, transgenic mice overexpressing ALS-associated SOD1 mutants develop ALS-like disease (5), and transgenic mice overexpressing human WT *SOD1* (*hwtSOD1*) or SOD1-deficient mice do not develop ALS-like disease (5, 6), suggesting that mutant SOD1 requires a threshold of expression to cause the disease through the gain of a toxic property.

Thus far, >100 mutations, widely distributed in the SOD1 polypeptide and involving >70 of its 153 codons, have been identified in ALS (www.alsod.org). It is not clear how diverse SOD1 mutants gain a common toxic property to cause ALS. Two types of hypotheses have been proposed (7). One focuses on the peroxidase-, superoxide reductase-, and superoxide-generating properties of mutant SOD1, leading to the formation of toxic species such as peroxynitrite, superoxide, and decomposition products of hydrogen peroxide. The other is derived from the observation of aggregates in ALS transgenic mice and patients (8–10), suggesting that the mutant SOD1 proteins are prone to form aggregates that may be toxic. The toxicity may also result from the loss of normal function of other proteins, caused by their entrapment in SOD1 aggregates.

The mutant protein aggregation hypothesis has been applied to several neurodegenerative disorders, and it has been variously argued that aggregates are causative, harmless, protective (11, 12), or even beneficial (7, 13). The relevance of these arguments to ALS and the fundamental molecular mechanism by which the SOD1 mutants form aggregates are not clear.

In the present study, we report the participation of hwtSOD1 in the pathogenic process whereby hwtSOD1 is recruited in the presence of mutant SOD1 and not only hastens disease in SOD1 mutant mice (*SOD1*$^{G93A}$ and SOD1$^{L126Z}$) but also converts a mutant transgenic mouse line (*SOD1*$^{A4V}$) from an unaffected phenotype to the typical clinical and pathological phenotype of ALS. Several convergent lines of evidence from our studies suggest that the molecular basis of these observations involves oxidation-mediated conversion of the soluble forms of both WT and mutant SOD1 into insoluble aggregates in the mitochondria, leading to the toxicity associated with ALS.

## Results

**hwtSOD1 Can Hasten Disease or Convert Transgenic Mice to an ALS-Like Phenotype.** We have previously shown that transgenic mice overexpressing an ALS-associated human SOD1 mutant with a G93A mutation (SOD1$^{G93A}$) develop ALS-like phenotype, but the transgenic mice overexpressing hwtSOD1 at similar or higher levels are phenotypically normal (5). We then studied the effect of overexpressed hwtSOD1 in mouse lines expressing three different SOD1 mutations (G93A, L126Z, and A4V). Our preliminary observation showed that hwtSOD1 hastens the ALS-like pheno-

Conflict of interest statement: No conflicts declared.

Freely available online through the PNAS open access option.

Abbreviations: hwt, human WT; ALS, amyotrophic lateral sclerosis.

†To whom correspondence may be addressed. E-mail: h-deng@northwestern.edu or t-siddique@northwestern.edu.

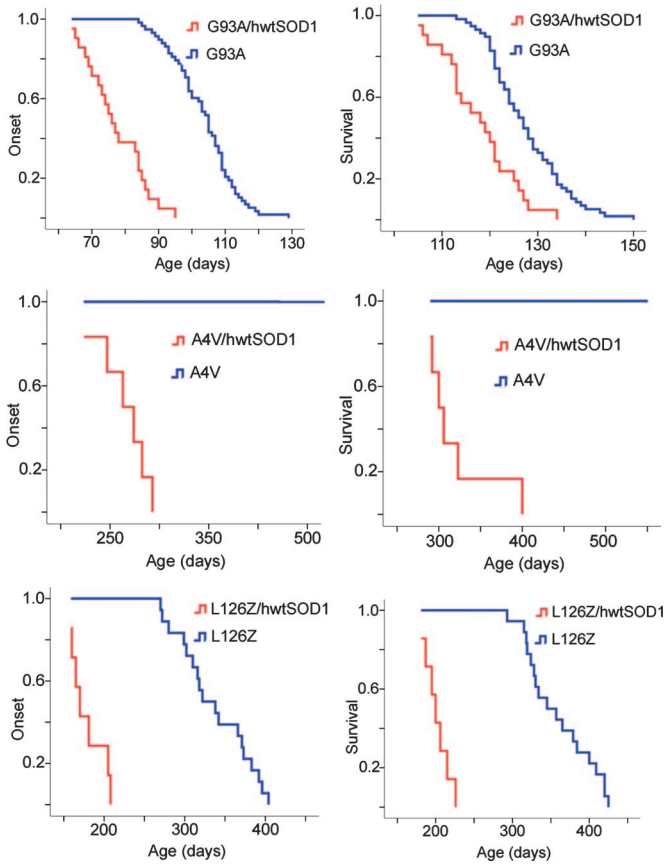


**Fig. 1.** Kaplan–Meier plots showing the age of onset and cumulative survival of the single- and double-transgenic mice. (*Top*) hwtSOD1 exacerbates the disease in $SOD1^{G93A}$ (shown as G93A) transgenic mice. The *G93A/hwtSOD1* double-transgenic mice (red line; $n = 21$) have an earlier onset of disease (76.8 ± 8.7 days vs. 103.2 ± 9.9 days; log-rank test $\chi^2 = 97.63$, $P < 0.0001$) (*Left*) and a shorter lifespan (117.7 ± 7.7 days vs. 127.4 ± 7.6 days; log-rank test $\chi^2 = 20.81$, $P < 0.0001$) (*Right*) than the *G93A* single-transgenic mice (blue line; $n = 58$, sibling control). (*Middle*) hwtSOD1 converts an unaffected phenotype of a $SOD1^{A4V}$ (shown as A4V) transgenic mouse line to an ALS-like phenotype. The *A4V* transgenic mice do not develop disease in their lifetime (>600 days; $n = 23$). However, the *A4V/hwtSOD1* double-transgenic mice ($n = 6$) *de novo* develop ALS-like disease (227.7 ± 50.7 days; $\chi^2 = 41.91$, $P < 0.0001$) (*Left*) with a shorter lifespan (318.5 ± 41.7 days; $\chi^2 = 41.01$, $P < 0.0001$) (*Right*). (*Bottom*) hwtSOD1 exacerbates the disease in $SOD1^{L126Z}$ (shown as L126Z) transgenic mice. The *L126Z/hwtSOD1* double-transgenic mice have a much earlier onset of disease [178.3 ± 19.1 days ($n = 7$) vs. 336.3 ± 42.7 days ($n = 18$); $\chi^2 = 34.38$, $P < 0.0001$] (*Left*) and a much shorter lifespan than the single-transgenic mice (201.4 ± 14.5 days vs. 359 ± 41.1 days; $\chi^2 = 34.38$, $P < 0.0001$) (*Right*).

type in $SOD1^{G93A}$ transgenic mice and shortens their lifespan (14). This observation was supported by a later study, even though fewer animals ($n = 4$) of a mouse line with a lower expression of mutant $SOD1^{G93A}$ were used (15). We repeated our experiment with a yet larger number of $SOD^{G93A}$ mice and confirmed our original findings (Fig. 1 *Top*).

We had also developed two lines of transgenic mice carrying human transgene $SOD1^{A4V}$ that do not develop disease even when aged to 2 years, probably on account of a lower expression of mutant $SOD1^{A4V}$ (5, 8). To test whether the hwtSOD1 could convert $SOD1^{A4V}$ mouse from an unaffected to an affected phenotype, we developed double-transgenic mice that overexpress both hwtSOD1 and $SOD1^{A4V}$. These $SOD1^{A4V}/hwtSOD1$ double-transgenic mice developed an ALS-like phenotype and died of the disease in <400 days (Fig. 1 *Middle*). We then crossed *hwtSOD1* transgenic with a second A4V transgenic line ($SOD1^{A4VL}$) with a lower expression level (20% compared with $SOD1^{A4V}$ based on RNA comparisons; data not shown) and found that these double-transgenic mice ($SOD1^{A4VL}/hwtSOD1$) did not develop ALS in their lifetime ($n = 3$), indicating that a threshold level of the mutant SOD1 is required for development of an ALS phenotype.

Because of similar molecular size and electrophoretic mobility of $SOD1^{G93A}$, $SOD1^{A4V}$, and hwtSOD1, it is technically difficult to distinguish hwtSOD1 from mutant SOD1 in aggregate preparations. Therefore, to distinguish mutant SOD1 from hwtSOD1 we developed a transgenic mouse model overexpressing a human SOD1 transgene with a premature stop codon at 126 ($SOD1^{L126Z}$) that had previously been reported by us in a familial ALS patient (16). $SOD1^{L126Z}$ is a truncated product that lacks the C-terminal 28 aa, and it can be easily differentiated from hwtSOD1 by electrophoretic mobility and antigenecity (*vide infra*). $SOD1^{L126Z}$ transgenic mice develop an ALS-like phenotype by the age of 300–400 days (17). This observation was later corroborated by other groups in $SOD1^{L126Z}$ and similar truncation mutations (18–20). To examine the effect of hwtSOD1 on $SOD1^{L126Z}$ mice, we developed $SOD1^{L126Z}/hwtSOD1$ double-transgenic mice and observed an earlier onset of disease and a shorter lifespan than $SOD1^{L126Z}$ single-transgenic mice (Fig. 1 *Bottom*). Thus, we concluded that hwtSOD1 not only hastens disease and shortens lifespan (G93A and L126Z) but also converts unaffected mutant SOD1 (A4V) transgenic mice to a disease phenotype, suggesting that not only the SOD1 mutants, but also the hwtSOD1, can participate in the pathogenesis of ALS. We then examined molecular correlates of this phenomenon.

**The Protein Aggregates Found in Affected Double-Transgenic Mice Contain both Mutant and WT SOD1.** Aggregates are observed in spinal cords of mutant *SOD1* mice (8–10), which eventually develop disease, but are not observed in *hwtSOD1* transgenic mice (5). We confirmed these observations using a SOD1 antibody (f-SOD1) raised against a full-length human SOD1 protein that reacts with both human and mouse SOD1. SOD1 immunoreactive aggregates were not observed in spinal cords of younger and unaffected $SOD1^{G93A}$ mice (<40 days) (Fig. 6 *a* and *b*, which is published as supporting information on the PNAS web site). No aggregates were observed in spinal cords of the unaffected $SOD1^{A4V}$ mice during the lifespan. But these aggregates were detected by our f-SOD1 antibody in the affected $SOD1^{A4V}/hwtSOD1$ double-transgenic mice. This convergence of phenotypic conversion and aggregate formation in $SOD1^{A4V}/hwtSOD1$ mice (Fig. 6 *c* and *d*) argues for the participation of hwtSOD1 in both of these apparently connected phenomena.

To investigate how hwtSOD1 may be involved in aggregate formation and to further characterize $SOD1^{L126Z}$ transgenic mice we developed two antibodies, one to discriminate between wtSOD1 (both human and mouse) and L126Z (c-SOD1 antibody), and a second antibody to discriminate between mouse and human SOD1 (hs-SOD1 antibody). The c-SOD1 antibody was raised by using a polypeptide consisting of the C-terminal 28 aa of human SOD1. It therefore recognizes both human and mouse SOD1, but not $SOD1^{L126Z}$; the hs-SOD1 antibody was raised by using a human-specific SOD1 polypeptide to recognize human SOD1 but not mouse SOD1 (*vide infra*). By immunostaining with the f-SOD1 antibody (which recognizes full-length SOD1), we found extensive aggregates in the gray matter of the spinal cord of affected $SOD1^{L126Z}$ mice (350 days) (Fig. 2*a*). When the c-SOD1 antibody was applied to spinal cord sections of the same $SOD1^{L126Z}$ affected mice, a diffuse staining pattern of endogenous mouse SOD1 was observed in activated astrocytes, but no aggregates were apparent (Fig. 2*b*). In immunostaining with the hs-SOD1 antibody, a pattern of abundant aggregates, rather than a diffuse staining pattern, was found (Fig. 2*c*) in affected mice but not in unaffected young mice (<5 months) (data not shown). These results suggested that the aggregated $SOD1^{L126Z}$ is the major pathogenic form of the trun-

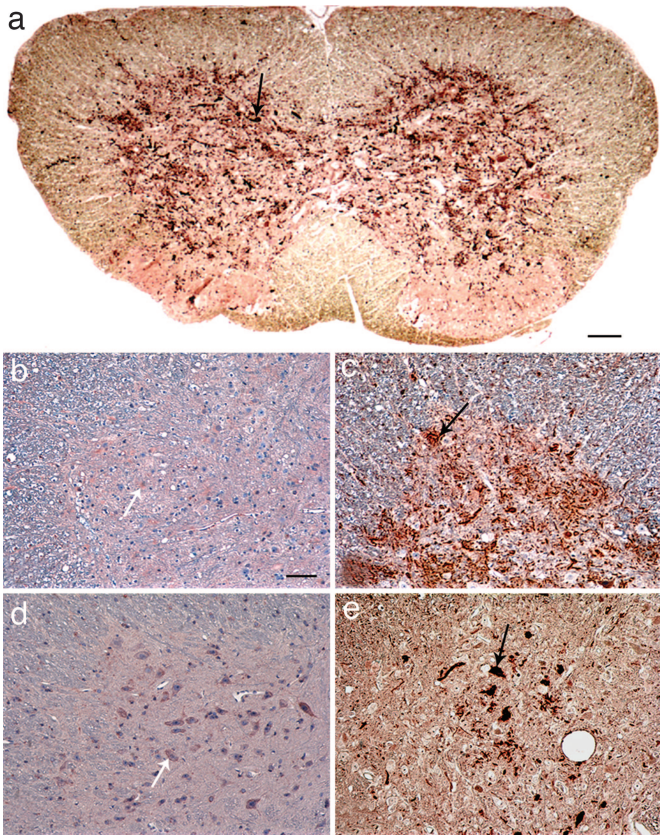


**Fig. 2.** Immunohistochemical staining of the spinal cord sections of various SOD1 transgenic mice. (*a–c*) *SOD1*$^{L126Z}$ mice, affected. (*a*) Distribution of SOD1-immunoreactive aggregates (arrow) in an entire spinal cord section, stained with the f-SOD1 antibody (not counterstained with hematoxylin for clarity of the distribution of the SOD1 aggregates). (Scale bar: 100 $\mu$m.) (*b*) c-SOD1 antibody: no aggregates and a light diffuse staining (arrow). (Scale bar: 35 $\mu$m.) (*c*) hs-SOD1 antibody, SOD1 aggregates of SOD1$^{L126Z}$, a component of the aggregates. A loss of the large neurons in the anterior horns is apparent in panels *a–c*. (*d*) *hwtSOD1* transgenic mice, unaffected. c-SOD1 antibody: diffusely distributed SOD1 immunostaining (arrow), predominantly in large cells, and no SOD1 aggregates in large neurons of the anterior horn of the spinal cord. (*e*) *SOD1*$^{L126Z}$/*hwtSOD1* double-transgenic mice, affected. c-SOD1 antibody: pronounced SOD1 aggregates (arrow), indicating the presence of wtSOD1 in the aggregates.

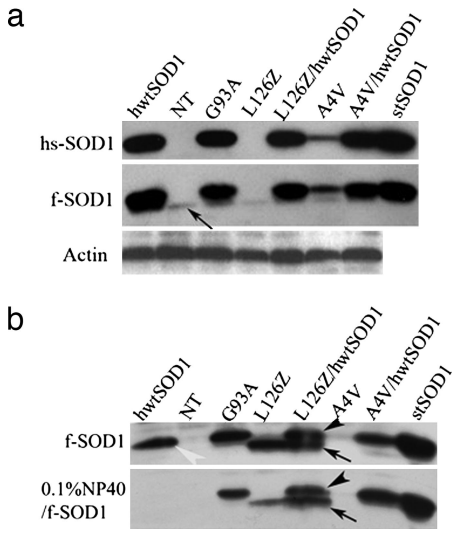


**Fig. 3.** Detergent-insoluble form of both mutant and WT SOD1 in spinal cord of affected transgenic mice. (*a*) SOD1 in the supernatant fraction detected with hs-SOD1 (*Top*) and f-SOD1 (*Middle*) antibodies in different mouse lines. NT, nontransgenic mice. $\beta$-Actin was used as a control (*Bottom*). Mouse endogenous SOD1 is indicated by an arrow. Human SOD1 is used as a standard (stSOD1). (*b*) SOD1 in the pellet fraction detected with f-SOD1 antibody. A certain amount of hwtSOD1 could be detected in *hwtSOD1* transgenic mice (*Upper*, arrowhead), but this hwtSOD1 is not detergent-insoluble (*Lower*). The detergent-insoluble form of SOD1 was detected in the affected *SOD1*$^{A4V}$/*hwtSOD1* double-transgenic mice but not in the unaffected *SOD1*$^{A4V}$ single-transgenic mice. The truncated SOD1$^{L126Z}$ protein was detected only in the insoluble fraction and was present in a detergent-insoluble form (arrow). Different from the hwtSOD1 in the *hwtSOD1* transgenic mice, the hwtSOD1 in the *SOD1*$^{L126Z}$/*hwtSOD1* double-transgenic mice is detergent-insoluble (arrowhead). Similar results were obtained by using the hs-SOD1 antibody.

cated SOD1 in the affected mice and underscores the relationship of aggregated form of mutant SOD1 to disease.

We observed the absence of SOD1 aggregation in the unaffected *SOD1*$^{A4V}$ mice and their presence in affected *SOD1*$^{A4V}$/*hwtSOD1* double-transgenic mice. In addition, the highly unstable SOD1$^{L126Z}$, although not detectable in the soluble (supernatant) form, was detected only in aggregated (pellet) form (Figs. 2 and 3, see below). Based on these observations, we hypothesized that hwtSOD1 exacerbates disease or converts to a disease phenotype through a mechanism in which the hwtSOD1 itself is converted from the physiological soluble form to an aggregated toxic form in the presence of mutant SOD1. We then tested this hypothesis using our *hwtSOD1*/*SOD*$^{L126Z}$ double-transgenic mice.

We have shown SOD1 aggregates in *SOD1*$^{L126Z}$ mice can be detected by using the hs-SOD1 and f-SOD1, but not c-SOD1 (Fig. 2). If hwtSOD1 is converted from a soluble form to an aggregated form in the *SOD1*$^{L126Z}$/*hwtSOD1* double-transgenic mice, then only hwtSOD1 (hwtSOD1 is $\approx$10-fold greater than the endogenous mouse SOD1 in the central nervous system of this transgenic line) would be detected in the aggregates with c-SOD1 antibody because it binds to the C terminus, absent in the L126Z protein. Consistent with this hypothesis, pronounced c-SOD1-positive aggregates were found in the *SOD1*$^{L126Z}$/*hwtSOD1* double-transgenic mice (Fig. 2*e*). SOD1-positive aggregates were not seen in control *hwtSOD1* transgenic mice (Fig. 2*d*). These data offer yet another line of evidence that hwtSOD1 is converted from a soluble form to an aggregated form in the double-transgenic mice and thereby contributes to exacerbation of disease.

To test whether mouse wtSOD1 participates in this pathogenic process, we generated *SOD1*$^{G93A}$ transgenic mice with mouse endogenous *SOD1* knocked out and observed a marginal delay of onset of disease and a longer lifespan (Fig. 7, which is published as supporting information on the PNAS web site), suggesting that both human and mouse wtSOD1 participate in the pathogenic process of the mutant SOD1-mediated disease in a dose-dependent manner. We did not detect apparent mouse SOD1 aggregates in *SOD1*$^{L126Z}$ mice using the c-SOD1 antibody (Fig. 2*b*), suggesting that the endogenous mouse SOD1 may be only a minor component in these aggregates and beyond the limits of detection with the c-SOD1 antibody and/or the detection system.

**Conversion of Mutant and WT SOD1 from a Soluble Form to an Aggregated and Detergent-Insoluble Form (SOD1$^{ADIS}$) Is Related to Its ALS-Associated Toxicity.** To characterize the biochemical property of aggregated SOD1, we first separated homogenates of spinal cords from different mice into two fractions using high-speed centrifugation (see *Supporting Materials and Methods*, which is published as supporting information on the PNAS web site). Proteins from each fraction were analyzed by Western blot by using SOD1 antibodies. In the supernatant fraction, both human SOD1 from the expression of the transgenes and mouse endogenous SOD1 that migrates ahead of the human SOD1 band were detected (Fig. 3*a*). In the pellet fraction we observed SOD1 in all of the

affected mice (Fig. 3*b*). A certain amount of hwtSOD1 from the *hwtSOD1* transgenic mice also appeared to be present in the pellet fraction (Fig. 3*b Upper*). However, this hwtSOD1 could be easily removed by washing with a mild detergent (0.1% Nonidet P-40) (Fig. 3*b Lower*), suggesting that SOD1 in the unaffected *hwtSOD1* transgenic mice is not detergent-insoluble. The $SOD1^{A4V}$ transgenic mice never develop ALS, and, as expected, $SOD1^{A4V}$ (using hs-SOD1 antibody) was detected in the supernatant fraction (Fig. 3*a*) and not in the pellet fraction (Fig. 3*b*). In contrast, SOD1 proteins in the affected $hwtSOD1/SOD1^{A4V}$ double-transgenic mice consistently remained in the pellet fraction even after treatment with a detergent (Fig. 3*b*). Because the $SOD1^{A4V}$ mice do not develop ALS-like symptoms in the absence of hwtSOD1 expression, these results again suggest that the detergent-insoluble form, rather than the soluble form, of SOD1 is associated with the disease.

Disease exacerbation and conversion to the ALS phenotype in our transgenic mouse models, in association with the expression of hwtSOD1, suggest involvement of hwtSOD1 in the formation of the disease-associated $SOD1^{ADIS}$. Because of the similar molecular size and electrophoretic property of the hwtSOD1 and $SOD1^{A4V}$, the contribution of each to $SOD1^{ADIS}$ cannot be identified in affected mice. We therefore took advantage of the smaller molecular size of $SOD1^{L126Z}$ in the $SOD1^{L126Z}$ transgenic mice. As shown in Fig. 3, the truncated $SOD1^{L126Z}$ protein was found in the detergent-insoluble fraction but was not detected in the soluble fraction. This result is consistent with our immunohistochemical study (Fig. 2 *a–c*) and indicates that the aggregated form of truncated SOD1 protein is detergent-resistant.

In the $hwtSOD1/SOD1^{L126Z}$ double-transgenic mice, hwtSOD1 was found in the supernatant fraction, as expected (Fig. 3*a*), but, interestingly, hwtSOD1 in the affected double-transgenic mice was also present in the pellet fraction (Fig. 3*b Upper*), was detergent-resistant (Fig. 3*b Lower*), and remained detergent-resistant despite harsher washing conditions (1% Nonidet P-40 and 1% Triton X-100; data not shown). This observation correlates with our immunohistochemical data that protein aggregates in the $hwtSOD1/SOD1^{L126Z}$ double-transgenic mice contain hwtSOD1 (Fig. 2*e*, and see below). The detergent-insolubility of hwtSOD1, therefore, represents a novel property of hwtSOD1 in the affected double-transgenic mice compared with the hwtSOD1 in the unaffected *hwtSOD1* mice.

**Both Mutant and WT SOD1 Participate in the Aggregate Formation in Mitochondria, Leading to Mitochondrial Damage.** SOD1 is predominantly a cytoplasmic enzyme (21), but it has also been detected in other cellular organelles, including mitochondria (22). Mutant SOD1 has been detected in mitochondria (15, 23) and reported to interact with the antiapoptotic protein Bcl-2 (24). The mutant SOD1 was also reported to form aggregates on the outer membranes of mitochondria (23, 25) and in the matrix (26). To test whether hwtSOD1 also forms aggregates in the spinal cord mitochondria of the affected mice, we examined spinal cord sections from the $hwtSOD1/SOD1^{L126Z}$ double-transgenic mice using the c-SOD1 antibody. Again, this antibody recognizes only wtSOD1 and not the truncated $SOD1^{L126Z}$. As shown in Fig. 8*f*, which is published as supporting information on the PNAS web site, dense gold particles were observed in mitochondria of the $hwtSOD1/SOD1^{L126Z}$ double-transgenic mice. The pattern of the SOD1 distribution is similar to that of the aggregated SOD1 in $SOD1^{G93A}$ mice in immunohistochemistry (Fig. 8 *a–e*). The dense signals were found in association with structures of both the outer and inner mitochondrial membranes, but especially with the inner membrane structures (Fig. 8*f*). Such dense signals were not detected in other organelles in the $hwtSOD1/SOD1^{L126Z}$ mice. We also observed that the cristae of the mitochondria with dense gold particles were severely damaged in the affected mice, including the $hwtSOD1/SOD1^{L126Z}$ (Fig. 8*f*), $SOD1^{G93A}$, and $SOD1^{L126Z}$ mice (Fig. 4). In the same mice, mitochondria with none or few gold particles appeared to be intact. (Fig. 4). Thus, formation of $SOD1^{ADIS}$ from both mutant and wtSOD1 in mitochondria, perhaps resulting in mitochondrial damage, is supported by our immunohistochemical, biochemical, and electron microscopy data (Figs. 2–4 and 8*f*).

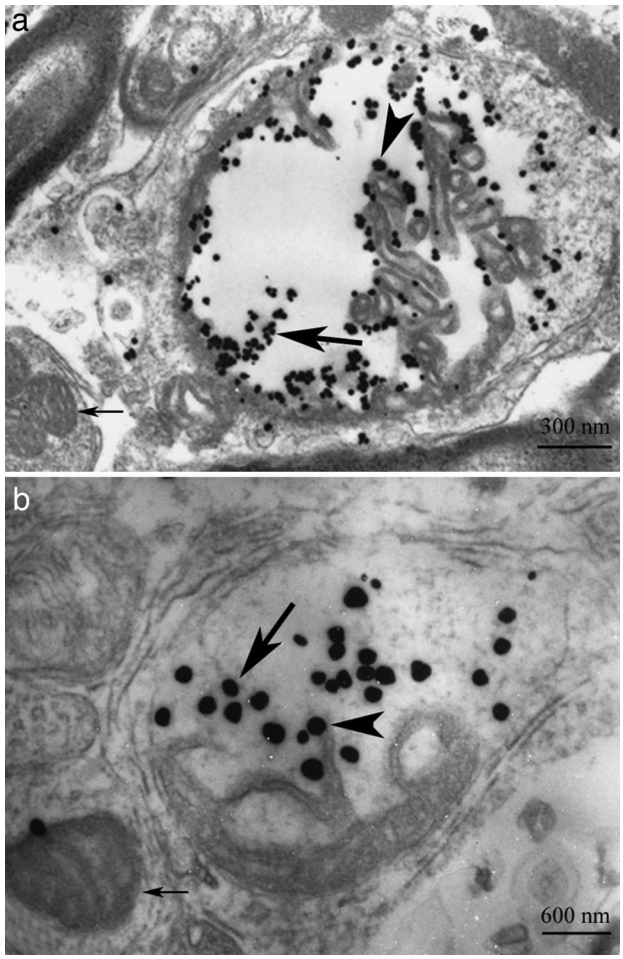


**Fig. 4.** ImmunoGold electron microscopy of the spinal cord sections with a SOD1 antibody (f-SOD1) showing altered mitochondrial morphology. The morphology of the cristae in gold-particle-dense areas was severely altered in the affected $SOD1^{G93A}$ (*a*) and $SOD1^{L126Z}$ (*b*) mice. Some gold particles were deposited in close association with the swollen cristae (arrowheads). Some cristae in the gold-particle-dense areas were severely damaged (large arrows). Such damage was not observed in the relatively normal mitochondria without (*a*) or with fewer (*b*) gold particles in the same mice as indicated by small arrows.

**Mutant and WT SOD1 Form Aggregates by Oxidation-Mediated Disulfide Crosslinking.** The mechanism by which $SOD1^{ADIS}$ is formed remains unclear. It has been proposed that the covalent crosslinking of SOD1 via the formation of intermolecular disulfides play a role in SOD1 aggregation *in vitro* (27, 28). However, it remains an open question whether such disulfide-linked SOD1 multimers physiologically correspond to the pathogenic aggregates found in spinal cord mitochondria. There are four cysteine residues in human SOD1 at amino acids 6, 57, 111, and 146, respectively, and formation of an intramolecular disulfide bond between Cys-57 and Cys-146 can stabilize and activate the protein in a physiological condition (27, 29). To test whether the SOD1 aggregates in the spinal cord mitochondria contain the intermolecular disulfide crosslinks, mitochondrial fraction was obtained from the spinal cords of affected transgenic mice and analyzed by using a method that modifies accessible cysteine residues with iodoacetamide (refs. 27 and 39).

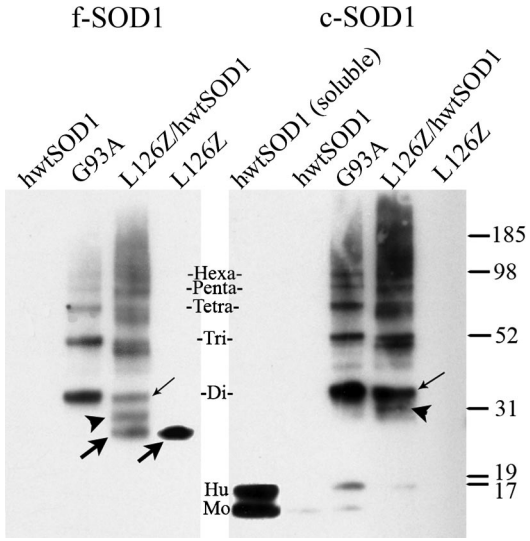


**Fig. 5.** Disulfide bond-mediated SOD1 dimers and multimers in the affected *SOD1*$^{G93A}$, *SOD1*$^{L126Z}$, and *SOD1*$^{L126Z}$/*hwtSOD1* mice. Shown are the detergent-insoluble mitochondrial fractions from transgenic mice overexpressing hwtSOD1, SOD1$^{G93A}$, SOD1$^{L126Z}$/hwtSOD1, and SOD1$^{L126Z}$. A soluble fraction from *hwtSOD1* transgenic mice [hwtSOD1 (soluble)] was also loaded to show the position of the human (Hu) and mouse (Mo) SOD1 monomers in *Right*. *Left* was detected with the antibody f-SOD1, and *Right* was detected with c-SOD1. Protein molecular weight markers are indicated on the right. The unaffected human *hwtSOD1* transgenic mice did not show SOD1 dimers and multimers, but affected *SOD1*$^{G93A}$ mice showed ladder-like SOD1 molecules, with the molecular sizes equivalent to dimer, trimer, tetramer, and so on, as labeled between *Left* and *Right*. The patterns of the dimers and multimers were similar, although two different antibodies (f-SOD1 and c-SOD1) were used. The affected *SOD1*$^{L126Z}$ mice showed a predominant dimer band when antibody f-SOD1 was applied. As expected, this dimer band was not detected by using the antibody c-SOD1 in *Right*. The *SOD1*$^{L126Z}$/*hwtSOD1* mice showed a unique pattern of dimers and multimers. The dimer group consisted of three dimer bands. The dimer band with the lower molecular weight (large arrow) in the *SOD1*$^{L126Z}$/*hwtSOD1* mice was similar to the dimer band in *SOD1*$^{L126Z}$ mice, in both molecular size and antigenecity with antibody c-SOD1, indicating that it is composed of the truncated SOD1$^{L126Z}$ protein. The dimer band with the higher molecular weight (small arrow) had a molecular size similar to that of the dimer in *SOD1*$^{G93A}$ mice, suggesting that two molecules of hwtSOD1, but not the truncated SOD1$^{L126Z}$, are involved in this dimer formation. The dimer band in the middle (arrowhead) was smaller than SOD1$^{G93A}$ dimer band but larger than SOD1$^{L126Z}$ dimer band in molecular size. It was positive when both the f-SOD1 and c-SOD1 were applied, but its intensity was greatly reduced with antibody c-SOD1. This finding suggests that it is a heterodimer, including one molecule unit of SOD1$^{L126Z}$ and one molecule unit of hwtSOD1. Apparently, each multimer group also consists of various combinations of hwtSOD1 and SOD1$^{L126}$ multimers. Very small amounts of SOD1 monomers could also be seen in longer time exposure as shown in *Right*.

As shown in Fig. 5, we found protein ladder-like SOD1-positive bands in the mitochondrial SOD1$^{ADIS}$ from the *SOD1*$^{G93A}$ mice. The molecular size of these bands corresponds to that of the SOD1 dimer, trimer, tetramer, and higher-order multimers.

The formation of dimers needs only one cysteine in each SOD1 molecule, but the formation of multimers requires at least two cysteine residues. To test whether Cys-146, which is deleted in SOD1$^{L126Z}$, is involved in the formation of the SOD1 dimers and multimers, we analyzed the SOD1$^{ADIS}$ from the *SOD1*$^{L126Z}$ mice. We found only one band with a molecular size corresponding to the dimers of the truncated SOD1$^{L126Z}$ (Fig. 5 *Left*). As expected, this dimer band was negative with the c-SOD1 antibody (Fig. 5 *Right*). These data suggest that two of the four cysteines in SOD1 are predominantly involved in the formation of the SOD1 dimers and multimers, one of which is Cys-146. The other highly reactive cysteine residue remains yet to be determined. But Cys-57 is likely, because it is a reactive cysteine and forms intramolecular disulfide bonds with Cys-146 in the physiological condition. Furthermore, recent *in vitro* studies suggested that Cys-57 and Cys-146 are more reactive for aggregate formation upon oxidation (refs. 28 and 39).

Unlike the *SOD1*$^{L126Z}$ mice, the *SOD1*$^{L126Z}$/*hwtSOD1* double-transgenic mice showed a large amount of higher-order multimers, which exhibit a slightly different size from those seen in *SOD1*$^{G93A}$ and are also detected by the c-SOD1 antibody (Fig. 5 *Right*). Three dimer bands were observed. Based on our analysis of the molecular weight and antigenicity of these dimers, they are apparently homodimers formed by two units of the truncated SOD1$^{L126Z}$, heterodimers formed by one unit of the truncated SOD1$^{L126Z}$ and one unit of the hwtSOD1, and homodimers formed by two units of the hwtSOD1 (Fig. 5). The other groups followed the same pattern (Fig. 5). Further biochemical characterization of these aggregates supports these findings (39). We thus conclude that both mutant and WT SOD1 can participate in the disulfide-linked aggregation.

## Discussion

In this report we describe a phenomenon whereby hwtSOD1 exacerbates ALS-like disease in *SOD1*$^{G93A}$ and *SOD1*$^{L126Z}$ transgenic mice and converts the state of unaffected *SOD1*$^{A4V}$ transgenic mice to ALS. This phenomenon is accompanied by a conversion of the hwtSOD1 from a soluble form to the SOD1$^{ADIS}$ in the presence of SOD1 mutants. These data therefore imply that the SOD1$^{ADIS}$ formed either by WT SOD1 or mutant or by both WT and mutant SOD1 are associated with disease. We further demonstrated that the SOD1$^{ADIS}$ aggregate consists of SOD1 dimers and multimers formed by intermolecular disulfide bonds via oxidation of cysteine residues in SOD1.

It is worth noting that wtSOD1 (both human and endogenous mouse SOD1) was reported not to show an obvious effect on disease onset in *SOD1*$^{G85R}$ mice (10). The reasons for this discrepancy are unclear. However, the lifespan of this line of *SOD1*$^{G85R}$ mice had a relatively large variation (ranging from 290 to 480 days) compared with the narrow variation in lifespan (127.4 $\pm$ 7.6 days) of our *SOD1*$^{G93A}$ mice. Such a large variation, together with relatively smaller sample size, may mask differences among different mouse groups. Closer examination of the survival plots of *SOD1*$^{G85R}$ and *SOD1*$^{G85R}$/*hwtSOD1* mice, which had a larger sample size, suggests a trend that *SOD1*$^{G85R}$/*hwtSOD1* mice had a shorter lifespan than *SOD1*$^{G85R}$ mice. Alternatively, this line of *SOD1*$^{G85R}$ mice may have a unique property that prevents or limits its interaction with wtSOD1.

Increased stability of mutant SOD1/hwtSOD1 heterodimers (noncovalent) has been proposed as a possible mechanism by which the wtSOD1 enhances the toxicity of mutant SOD1 (30). The C-terminal truncated mutants, including SOD1$^{L126Z}$, which lack the C-terminal active loop VII, is unable to form homodimers or heterodimers with wtSOD1 (16, 18). However, hwtSOD1 still enhances SOD1$^{L126Z}$ toxicity, suggesting that noncovalent heterodimer stabilization of mutant SOD1 is unlikely to be a mechanism by which wtSOD1 enhances mutant SOD1 toxicity.

The disulfide-reduced form of SOD1 monomers has been suggested to be an intermediate in the aggregation process (28, 31). This reduced form of monomers was shown to be the only eligible form to be transported into mitochondria (32). The reduced form of SOD1 was recently demonstrated to be enriched in the susceptible tissues of transgenic mice (33). Compared with wtSOD1, ALS-associated mutant SOD1 proteins have increased susceptibility to reduction of the intramolecular disulfide bond (34). The accessible cysteines can be modified by oxidative stress, leading to disulfide-linked multimerization of SOD1 *in vitro*/*in vivo* (refs. 27, 28, and 39). Based on this information and our findings, we propose that mutations in SOD1 may destabilize SOD1 *in vivo* (4), interfering with the formation of the intramolecular disulfide bond between Cys-57 and Cys-146 and leading to an increased amount of the reduced form of SOD1 proportionally; this reduced form of

SOD1 has an increased accessibility to subcellular compartments such as mitochondria (32), where a fraction of the reduced monomer forms dimers and multimers by intermolecular disulfide bonds; these dimers and multimers are insoluble and may interfere with the normal function of the organelles and the cells, eventually leading to neuronal degeneration. It is also expected that a fraction of wtSOD1 is in a disulfide-reduced form, albeit much less than that of ALS-associated mutant proteins proportionally. The amount of the disulfide-reduced wtSOD1 is increased when it is highly expressed, as in the *hwtSOD1* transgenic mice. The reduced wtSOD1 can be transported into mitochondria, where it forms insoluble heterodimers and heteromultimers with the mutant SOD1 or wtSOD1 homodimer and multimers upon oxidative stress, because the oxidative aggregation propensity was also shown in wtSOD1 *in vitro* (28).

Aggregated proteins or inclusions are a pathological hallmark of some neurodegenerative disorders (35). Oxidation has been suspected to play an important role in normal aging process and in the pathogenesis of these neurodegenerative disorders (36, 37). However, the relationship among protein oxidation, protein aggregation, and neurodegeneration remains unclear (36, 37). The oxidative intermolecular disulfide crosslinking paradigm presented here provides direct links among protein oxidation, protein aggregation, and neurodegeneration in SOD1-mediated ALS. This mechanism may play an important role not only in the SOD1-mediated ALS but also in some other neurodegenerative disorders. For example, prion protein also has a conserved intramolecular disulfide bond, and the formation of intermolecular disulfide bonds was suggested for seeded conversion of recombinant prion protein by an *in vitro* study (38).

Based on our findings that ALS-associated aggregates are, in part, composed of insoluble SOD1 dimers and multimers formed by intermolecular disulfide bonds via oxidation of cysteine residues in SOD1, the two current apparently disparate hypotheses of ALS pathogenesis (oxidation and aggregation) can be reconciled. This reconciliation is evident when considering that an increased oxidative stress may enhance the formation of the oxidized insoluble SOD1 aggregates. Finally, these findings lay a rational basis to design therapies that interrupt interaction of unstable and improperly folded proteins with redox mechanisms in specific cell organelles.

## Materials and Methods

**Development of Transgenic Mice Overexpressing the Human Mutant SOD1$^{L126Z}$.** The L126Z mutation was introduced into exon 5 of the human SOD1 gene by site-directed mutagenesis with PCR by using a 7-kb PvuII/BamHI fragment containing exons 2–5 in a plasmid vector as a template. The entire transgene was assembled by ligation of the 4.6-kb EcoRI/PvuII fragment containing exon 1 and the 7-kb PvuII/BamHI fragment containing the L126Z mutation into pBluescript plasmid vector. The 11.6-kb EcoRI/BamHI transgene was used for microinjection into fertilized eggs. Transgenic mice were identified by both PCR and Southern blot analysis. The animal and animal use protocols have been approved by the Institutional Animal Care and Use Committee of Northwestern University.

**Detection of SOD1 Dimers and Multimers.** Fresh preparations of mouse spinal cords were homogenized in homogenizing buffer (50 mM Hepes/1 mM EDTA/100 mM iodoacetamide, pH 7.2). The homogenate was incubated at 37°C for 1 h and was subjected to centrifugation at 200 $\times$ *g* for 5 min to remove the nuclei and unbroken cells. The mitochondria fraction was prepared by using sucrose and Percoll protocols. The mitochondrion-enriched fraction was pelleted and washed six times with buffer containing 50 mM Hepes, 1 mM EDTA, 100 mM iodoacetamide (pH 7.2), and 0.1% Nonidet P-40 and analyzed by Western blot analysis by using 4–12% Bis-Tris gel without reductants.

Details regarding development of transgenic mice, antibody production, Western blot analysis, histopathological analysis, confocal microscopy, and immunoelectron microscopy are in *Supporting Materials and Methods*.

This study was supported by National Institute of Neurological Disorders and Stroke Grants NS40308 (to H.-X.D.), NS050641 (to T.S.), and NS046535 (to T.S.); the Les Turner ALS Foundation (T.S.); the Amyotrophic Lateral Sclerosis Association (H.-X.D.), National Institute of General Medical Sciences Grant 54111 (to T.V.O.); a Japan Society for the Promotion of Science Postdoctoral Fellowship for Research Abroad (to Y.F.); the National Organization for Rare Disorders; the Vena E. Schaff ALS Research Fund; a Harold Post Research Professorship; the Herbert and Florence C. Wenske Foundation; the Ralph and Marian Falk Medical Research Trust; an Abbott Labs Duane and Susan Burnham Professorship; and the David C. Asselin MD Memorial Fund (T.S.).

1. Hughes, J. T. (1982) *Adv. Neurol.* **36,** 61–74.
2. Lacomblez, L., Bensimon, G., Leigh, P. N., Guillet, P. & Meininger, V. (1996) *Lancet* **347,** 1425–1431.
3. Rosen, D. R., Siddique, T., Patterson, D., Figlewicz, D. A., Sapp, P., Hentati, A., Donaldson, D., Goto, J., O'Regan, J. P., Deng, H.-X., *et al.* (1993) *Nature* **362,** 59–62.
4. Deng, H.-X., Hentati, A., Tainer, J. A., Iqbal, Z., Cayabyab, A., Hung, W. Y., Getzoff, E. D., Hu, P., Herzfeldt, B., Roos, R. P., *et al.* (1993) *Science* **261,** 1047–1051.
5. Gurney, M. E., Pu, H., Chiu, A. Y., Dal Canto, M. C., Polchow, C. Y., Alexander, D. D., Caliendo, J., Hentati, A., Kwon, Y. W., Deng, H.-X., *et al.* (1994) *Science* **264,** 1772–1775.
6. Reaume, A. G., Elliott, J. L., Hoffman, E. K., Kowall, N. W., Ferrante, R. J., Siwek, D. F., Wilcox, H. M., Flood, D. G., Beal, M. F., Brown, R. H., Jr., *et al.* (1996) *Nat. Genet.* **13**, 43–47.
7. Liochev, S. I. & Fridovich I. (2003) *Free Radical Biol. Med*. **34,** 1383–1389.
8. Dal Canto, M. C. & Gurney, M. E. (1995) *Brain Res.* **676,** 25–40.
9. Shibata, N., Hirano, A., Kobayashi, M., Siddique, T., Deng, H.-X., Hung, W. Y., Kato, T. & Asayama, K. (1996) *J. Neuropathol. Exp. Neurol.* **55,** 481–490.
10. Bruijn, L. I., Houseweart, M. K., Kato, S., Anderson, K. L., Anderson, S. D., Ohama, E., Reaume, A. G., Scott, R. W. & Cleveland, D. W. (1998) *Science* **281,** 1851–1854.
11. Cleveland, D. W. & Liu, J. (2000) *Nat. Med.* **6,** 1320–1321.
12. Bruijn, L. I., Miller, T. M. & Cleveland, D. W. (2004) *Annu. Rev. Neurosci.* **27**, 723–749.
13. Sherman, M. Y. & Goldberg, A. L. (2001) *Neuron* **29**, 15–32.
14. Deng, H.-X., Fu, R. & Siddique, T. (1998) *Am. J. Hum. Genet. Suppl.* **63,** A2069.
15. Jaarsma, D., Haasdijk, E. D., Grashorn, J. A., Hawkins, R., Van Duijn, W., Verspaget, H. W., London, J. & Holstege, J. D. (2000) *Neurobiol. Dis.* **7,** 623–643.
16. Zu, J. S., Deng, H.-X., Lo, T. P., Mitsumoto, H., Ahmed, M. S., Hung, W.-Y., Cai, Z. J., Tainer, J. A. & Siddique, T. (1997) *Neurogenetics* **1,** 65–71.
17. Deng, H.-X., Fu, R., Zhai, H. & Siddique, T. (1999) *Am. J. Hum. Genet. Suppl.* **65,** A1636.
18. Jonsson, P. A., Ernhill, K., Andersen, P. M., Bergemalm, D., Brannstrom, T., Gredal, O., Nilsson, P. & Marklund, S. L. (2004) *Brain* **127,** 73–88.
19. Watanabe, Y., Yasui, K., Nakano, T., Doi, K., Fukada, Y., Kitayama, M., Ishimoto, M., Kurihara, S., Kawashima, M., Fukuda, H., *et al.* (2005) *Brain Res. Mol. Brain Res.* **135,** 12–20.
20. Wang, J., Xu, G., Li, H., Gonzales, V., Fromholt, D., Karch, C., Copeland, N. G., Jenkins, N. A. & Borchelt, D. R. (2005) *Hum. Mol. Genet.* **14,** 2335–2347.
21. Weisiger, R. A. & Fridovich, I. (1973) *J. Biol. Chem.* **248,** 3582–3592.
22. Chang, L. Y., Slot, J. W., Geuze, H. J. & Crapo, J. D. (1988) *J. Cell Biol.* **107,** 2169–2179.
23. Higgins, C. M., Jung, C. & Xu, Z. (2003) *BMC Neurosci.* **4,** 16.
24. Pasinelli, P., Belford, M. E., Lennon, N., Bacskai, B. J., Hyman, B. T., Trotti, D. & Brown, R. H., Jr. (2004) *Neuron* **43**, 19–30.
25. Liu, J., Lillo, C., Jonsson, P. A., Vande Velde, C., Ward, C. M., Miller, T. M., Subramaniam, J. R., Rothstein, J. D., Marklund, S. L., Andersen, P. M., *et al*. (2004) *Neuron* **43,** 5–17.
26. Vijayvergiya, C., Beal, M. F., Buck, J. & Manfredi, G. (2005) *J. Neurosci.* **25,** 2463–2470.
27. Furukawa, Y., Torres, A. S. & O'Halloran, T. V. (2004) *EMBO J.* **23,** 2872–2881.
28. Furukawa, Y. & O'Halloran, T. V. (2005) *J. Biol. Chem.* **280,** 17266–17274.
29. Lepock, J. R., Frey, H. E. & Hallewell, R. A. (1990) *J. Biol. Chem.* **265,** 21612–21618.
30. Fukada, K., Nagano, S., Satoh, M., Tohyama, C., Nakanishi, T., Shimizu, A., Yanagihara, T. & Sakoda, S. (2001) *Eur. J. Neurosci.* **14,** 2032–2036.
31. Rakhit, R., Crow, J. P., Lepock, J. R., Kondejewski, L. H., Cashman, N. R. & Chakrabartty, A. (2004) *J. Biol. Chem.* **279,** 15499–15504.
32. Field, L. S., Furukawa, Y., O'Halloran, T. V. & Culotta, V. C. (2003) *J. Biol. Chem.* **278,** 28052–28059.
33. Jonsson, P. A., Graffmo, K. S., Andersen, P. M., Brannstrom, T., Linderberg, M., Oliverberg, M. & Marklund, S. L. (2006) *Brain* **129,** 451–464.
34. Tiwari, A. & Hayward, L. J. (2003) *J. Biol. Chem.* **278,** 5984–5992.
35. Taylor, J. P., Hardy, J. & Fischbeck, K. H. (2002) *Science* **296**, 1991–1995.
36. Butterfield, D. A. & Kanski, J. (2001) *Mech. Ageing Dev.* **122**, 945–962.
37. Beal, M. F. (2002) *Free Radical Biol. Med.* **32**, 797–803.
38. Lee, S. & Eisenberg, D. (2003) *Nat. Struct. Biol.* **10,** 725–730.
39. Furukawa, Y., Fu, R., Deng, H.-X., Siddique, T. & O'Halloran, T. V. (2006) *Proc. Natl. Acad, Sci. USA,* in press.